Contents list available at CBIORE journal website

International Journal of Renewable Energy Development

Journal homepage: https://ijred.cbiore.id

Research Article

Integrated multi-objective optimization of fuel injection and engine strategy in oxyhydrogen/producer gas-powered dual-fuel diesel engine

Du Nguyen[a], Lan Huong Nguyen[b], Duy Tan Nguyen[c], Nghia Chung[c], Thanh Hai Truong[c,*]

[a]*Institute of Engineering, HUTECH University, Ho Chi Minh City, Vietnam.*

[b]*School of Mechanical Engineering, Vietnam Maritime University, Haiphong, Vietnam.*

[c]*Institute of Maritime, Ho Chi Minh City University of Transport, Ho Chi Minh City, Viet Nam*

Abstract. Biomass gasification has taken on a new significance as a decentralized and sustainable route of turning solid biomass into oxyhydrogen (HHO) enriched producer gas that can be employed in internal combustion engines using diesel as the pilot fuel. This dual fuel system can cut down on reliance on fossil diesel as well as improve the energy security of rural and semi-urban applications. This study examines the engine operation and emissions characteristics of the producer-gas-diesel dual-fuel engine under the main operating parameters and uses statistical optimization to reduce the emissions and still attain acceptable efficiency. Indeed, Prosopis juliflora wood gasification was conducted in a small, fixed-bed downdraft gasifier, which is only intended to be used in decentralized and experimental engines. Downdraft design was chosen because of the intrinsic effect that it provides low-tar PG, which must be supplied to internal combustion engines. The optimization findings reveal that the maximum brake mean effective pressure (BMEP) is 4.23 bar, pilot fuel injection pressure (PFIP) is 240 bar, and HHO flow rate (HHOFR) is 2.08 LPM. The predicted values of Brake Thermal Efficiency (BTE), Brake Specific Energy Consumption (BSEC), and carbon monoxide (CO), hydrocarbons (HC), and nitrogen oxides (NOx) emissions at these settings are estimated to be 20.71 %, 4.17 MJ/kWh, and 77.95, 79.47, and 335.99 ppm, respectively. The findings indicate that the balance between the supply of producer gas and the optimization of injection parameters can greatly enhance the sustainability and emission characteristics of the dual-fuel engine running on gaseous fuel that is produced from biomass.

Keywords: Biomass gasification, Producer gas, Sustainability, Alternative fuel, Dual-fuel diesel engine

Received: 14st August 2025; Revised: 30th Oct 2025; Accepted: 05th November 2025; Available online: 28th Dec 2025

1. Introduction

Biomass has become one of the most significant renewable energy sources to help solve the growing energy demand of the world. In the present era, there is an urgent need to decrease the reliance on fossil fuels and the emission of greenhouse gases (GHGs) (V. G. Nguyen *et al.*, 2024; Sharma *et al.*, 2025). Owing to abundant availability, carbon neutrality, and suitability with the current energy conversion packages, biomass is a sustainable alternative to replace fossil fuels (Nguyen & Le, 2023). This option becomes more attractive in the developing countries, where agricultural remnants, forest waste, and organic by-products are abundant (Phrommarat & Arromdee, 2025; Santana *et al.*, 2025). Among the biomass-to-energy routes, there has been considerable interest in thermochemical conversion, or biomass gasification. The biomass gasification process can allow low-grade solid biomass to be converted efficiently into a clean, combustible gaseous fuel which can be directly used in internal combustion engines (ICEs), in gas turbines, and in combined heat and power systems (Le *et al.*, 2024; Sharma & Bora, 2023). In biomass gasification, solid biomass is used to produce a producer gas, which is primarily a mixture of CO, H_2, CH_4, CO_2, and N_2 as a result of controlled partial oxidation at high temperatures (Huynh *et al.*, 2025; Prajapati & Tirkey, 2025). Although this gaseous fuel has a lower calorific value than conventional hydrocarbons, it has good ignition properties when it is combined with a high reactivity pilot fuel like diesel (Prajapati *et al.*, 2024; Raj *et al.*, 2024; Reyes *et al.*, 2024). Producer gas is not only easier to clean and transport compared to the raw biomass, but also offers more stable combustion, less formation of particulate, and lower net carbon emission (P. Q. P. Nguyen *et al.*, 2025). With nations in the process of implementing aggressive decarbonization policies, the use of biomass gasification technology with ICEs offers a stable and affordable path to decentralized renewable energy production, especially in rural or remote areas (Chermprayong *et al.*, 2024; Monteiro *et al.*, 2024; Prabhahar *et al.*, 2024).

Although electrification gains greater importance, diesel engines remain of essential importance in transportation, agricultural, and decentralized power systems because of their durability, high thermal efficiency, fuel flexibility, and capacity to be utilized in variable-loading situations (Hoang, 2019; Veza *et al.*, 2022). Nonetheless, diesel engines are not free of severe environmental problems such as the release of nitrogen oxides (NOx), particulate matter (PM), unburnt hydrocarbons, and CO_2

* Corresponding author
Email: hai.truong@ut.edu.vn (T.H. Truong)

https://doi.org/10.61435/ijred.2026.62062
ISSN: 2252-4940/© 2026.The Author(s). Published by CBIORE

(Hoang, 2024). Newer international standards of emissions and the long-term sustainability of petroleum-based fuels have increased the demand for cleaner combustion approaches without jeopardizing the engine life or its stability in operation (Le *et al*., 2025; Palani *et al*., 2020; Zhang *et al*., 2023). The traditional diesel burning, though efficient, is limited by the chemistry of its fuels, high temperatures in the in-cylinder, and the soot-NOx trade-offs, which are hard to break without significant changes or post-treatment equipment (Barik & Murugan, 2014; Ma *et al*., 2026; Stettler *et al*., 2016). The concept of dual-fuel operation has become a promising technology to address these issues with the enablement of low-reactivity alternative fuels to replace much of the diesel with the stable ignition and consistent combustion by a small pilot injection of diesel (Liu *et al*., 2015; Shu *et al*., 2022; Winangun *et al*., 2023). In dual-fuel engines, the fuel gases like producer gas, biogas, natural gas, or hydrogen gas can be added in the intake air stream, with a benign amount of diesel (termed as pilot fuel) injected directly into the cylinder around top dead center to initiate the combustion (Das *et al*., 2022; Sharma *et al*., 2023; Singh *et al*., 2021). This plan saves on the total amount of diesel used as well as increasing the flexibility of fuel, lowering the carbon intensity, and lowering the amount of particulate emission as a result of the relatively cleaner combustion of the gaseous fuels. In addition, the dual-fuel systems may be installed in a currently existing diesel engine with very few hardware changes, and this makes it economically viable and technologically feasible to apply the technology on a large scale (Bora & Saha, 2016; Krop & Brito, 2023; V. N. Nguyen, Nayak, *et al*., 2023).

Recent studies offer credible experimental support to the conclusion that producer gas (PG) can become the main energy carrier in diesel-producer-gas dual-fuel systems, and offer significant fuel replacement and emission offset advantages with reasonably manageable trade-offs in efficiency and combustion stability (Caligiuri *et al*., 2023; Raj *et al*., 2024). Indeed, Halewadimath *et al*. (Halewadimath *et al*., 2020) reported that hydrogen-enriched PG in a CRDI diesel engine-operating on biodiesel pilot fuel increased brake thermal efficiency slightly and generated significant decreases in smoke, HC, and CO, but at some setups had an intermediate rise in NOx. Caligiuri *et al*. (Caligiuri *et al*., 2021) explored the PG produced through forestry and supplied to micro-CHP and engine operation, and found that by attentively coordinating the process of gasifier operation, gas cleaning, and engine control, the extent of diesel replaced by the gas can be high with significant decreases in the intensity of particulate and CO_2 emissions. In another study by Caligiuri *et al*. (Caligiuri *et al*., 2023), they further expanded the data-driven optimization tools to manage the NOx-soot trade-off in practice in deploying PG-powered micro-CHP. Percy *et al*. (Percy & Edwin, 2023) experimented on a variable-compression-ratio diesel engine fueled by PG and demonstrated that dual-fuel operation can offer significant diesel savings when compression and injection parameters are optimized, without a significant compromise in combustion stability at medium-to-high loads. These studies published in last five years also highlight the key role of strict multi-stage gas cleaning, cooling as well as engine tuning: various published articles have reported diesel substitution levels generally in the 20-60% range based on feedstock and load, as well as repeated reports of higher CO/HC at low loads and efficiency costs without optimizing injection timing and pilot quantity. Together, the published literature illustrates PG-diesel dual-fuel technology as a feasible path to decentralized, low-carbon power when combined with aggressive gasifier design, extensive cleaning/cooling, and optimized injection/control plans to reconcile fuel savings, emissions reduction, and engine performance. However, the use of PG has several challenges, such as low flame speed, high cyclic variability, and low lean-burn stability, which all contribute to reduced efficiency and incomplete-combustion emissions (Chanphavong & Zainal, 2019; Nayak *et al*., 2021). The addition of hydrogen (H_2) or oxy-hydrogen (HHO) to PG-fueled engines has been found to overcome these challenges to a certain extent. The high calorific value of H_2 and HHO could improves the reactivity of the mixtures, ignition stability, and offsets low-calorific PG to cleaner and more efficient operation (Bui *et al*., 2025; Khandal *et al*., 2022). As such, HHO-enriched PG-diesel dual-fuel engines represent the best of both worlds and the PG biomass environmental benefits, and the reliability of diesel engines. The interaction of PG properties and influencing engine parameters like injection pressure, quantity of pilot fuel, and load conditions is very crucial to combustion phasing, ignition delay, flame propagation, and overall performance. Consequently, fuel injection and operating strategy optimization are necessary to improve performance and reduce emissions during dual-fuel operation. The use of multi-objective optimization methods offers a very strong framework of systematic assessment of these interacting variables and a determination of the most efficient trade-offs between performance, fuel economy, and environmental impact. The paper presents research on the creation of an optimized strategy of a diesel engine that performs in the dual-fuel mode with the help of PG.

2. Materials and Methods

2.1 Producer gas feedstock

In this investigation, Prosopis juliflora wood has been used as the main biomass feedstock in the generation of PG. This variety of wood is relatively easy to get in semi-arid and rural areas, the calorific value is relatively high, and it has low sulphur and moderate ash content, which makes it very appropriate for small-scale gasification plants. The homogeneous structure and composition provide stable thermal decomposition and PG

Table 1
Main properties of the test fuel

Property	Prosopis juliflora wood (biomass)	Diesel fuel (liquid)
State	Solid wood chips/pieces	Liquid hydrocarbon
Moisture content (wt%)	12 to 16 (as received)	-
Volatile matter (wt%, db)	74	-
Fixed carbon (wt%, db)	14.5	–
Ash content (wt%, db)	2.5	<0.01
Higher heating value	18400 MJ/kg	42400 MJ/kg
Bulk density	289 kg/m³	844 kg/m³
Carbon (wt%, db)	47	-
Hydrogen (wt%, db)	5.4	-
Oxygen (wt%, db)	43.5	-
Sulfur (wt%)	<0.05	-
Typical use in this study	Gasifier feedstock for producer gas	Pilot fuel in dual-dual-fuel CI engine

quality even under continuous operation (Ghodke & Mandapati, 2019; Huynh *et al*., 2025). The wood was milled to attain a uniform particle size of about 25 to 35 mm before being dried. It was ensured that the wood had moisture levels up to 12% before entering the gasification unit. The low moisture level is important to avoid the occurrence of gasifier channeling, back-firing, and tar excess. The use of Prosopis juliflora wood as the feedstock, therefore, adds directly to cleaner combustion, better PG calorific value, and consistency of the operation of the dual-fuel diesel engine (Bandara *et al*., 2022; Oduor & Githiomi, 2013). The main properties of fuel tested in this study are listed in Table 1.

2.2. Biomass gasification in a downdraft gasifier

Biomass gasification occurs in a gasifier where the feedstock is exposed to intense heat, resulting in the chemical transformation of the feedstock to gaseous fuels (Tulu *et al*., 2022). Prosopis juliflora wood gasification was conducted in a small, fixed-bed downdraft gasifier, which is only intended to be used in decentralized and experimental engines. Downdraft design was chosen because of the intrinsic effect that it provides low-tar PG, which must be supplied to internal combustion engines (Huang *et al*., 2019). Biomass is transported to the bottom of such a system by a series of reaction zones: drying, pyrolysis, oxidation, and reduction, which are caused by gravity and the controlled flow of air (Patra & Sheth, 2015; Susastriawan *et al*., 2017). As the feedstock falls, it is first dried, and then it is pyrolyzed, where moisture is removed, and volatile matter is set free. High-temperature partial combustion is facilitated by adding air towards the oxidation area, and this supplies the thermal energy needed in the subsequent endothermic gasification reactions (Havilah *et al*., 2022). The char bed in the reduction zone below enables the important reactions to occur; these include the Boudouard reaction ($C + CO_2 = 2CO$) (Dai *et al*., 2021; Lahijani *et al*., 2015), water-gas reaction ($C + H_2O = CO + H_2$) (Chen & Chen, 2020; Smith R J *et al*., 2010), and methane formation. The effect is the production of a PG that is mainly made up of CO, H_2, and a small amount of traces of CH_4 and other dilution gases such as CO_2 and N_2. Since the gas must move through the layer of hot char before leaving the reactor, the downdraft design reduces tar content over updraft designs. In dual-fuel diesel engines, much tar would result in large intake manifolds, injector deposits, and unstable combustion, showing that the small downdraft gasifier is appropriate.

2.3 Gas cleaning and cooling

Raw PG produced in the gasifier has particulate matter, fine char, ash, condensable tar vapors, and moisture, which should be eliminated in order to achieve smooth and reliable engine operation. To ensure this, a gas cleaning and cooling system in several stages was adopted. The gas is initially subjected to a cyclone separator- the inertial forces separate coarse particulate matter and char dust (Asadullah, 2014; Thomson *et al*., 2020). It is then pressure-to-wet scrubbed or washed in a water-based cleaning device, which serves to condense tar vapors and trap fine particles suspended in the gas stream. After primary cleaning, the gas is passed through a gas cooler or heat exchanger to cool the gas to a reasonable temperature so as to permit it into the engine. Cooling is also known to enhance the density and combustion properties of the gas and to condense any tar droplet that is left behind (Freda *et al*., 2024; Sutar *et al*., 2023). In order to provide the diesel engine with clean, consistent, high-quality PG, the gas undergoes a last fine-filtration stage utilizing a sawdust filter, cloth filter, or activated carbon bed to eliminate any leftover contaminants. The engine's valves, piston rings, and injection system are secured by this cleaning and cooling process, which also prevents malfunctions like misfiring or knocking and ensures steady dual-fuel combustion throughout test activities (Das *et al*., 2020; Raman *et al*., 2013).

2.4 Test engine

The power-generation unit uses a single-cylinder, four-stroke, variable compression ratio diesel engine, with the two-fuel option, with a maximum brake power of approximately 3.75 kW at 1500 + 50 rpm. By changing the cylinder head setting, the engine compression ratio can be set to 12 or 22. Intake is pre-mixed with PG in a T-junction manifold, and the rate of gas and air flow is measured using single flow meters. Pilot fuel is supplied by an auxiliary diesel tank, injected at a conventional diesel injector at an injection pressure of 200 bar. The power is absorbed by an eddy-current dynamometer connected to the crankshaft. The engine load can be varied and measured between zero and the rated load of 3.75 kW using a manually loaded strain-gauge-based electrical loading unit with voltage and current indicators. The rotational speed of the engine is monitored using a digital laser tachometer. Gaseous emissions at the exhaust are measured with the AVL Digas 444 analyzer, which can measure concentrations of CO, HC, and NOx. Diesel

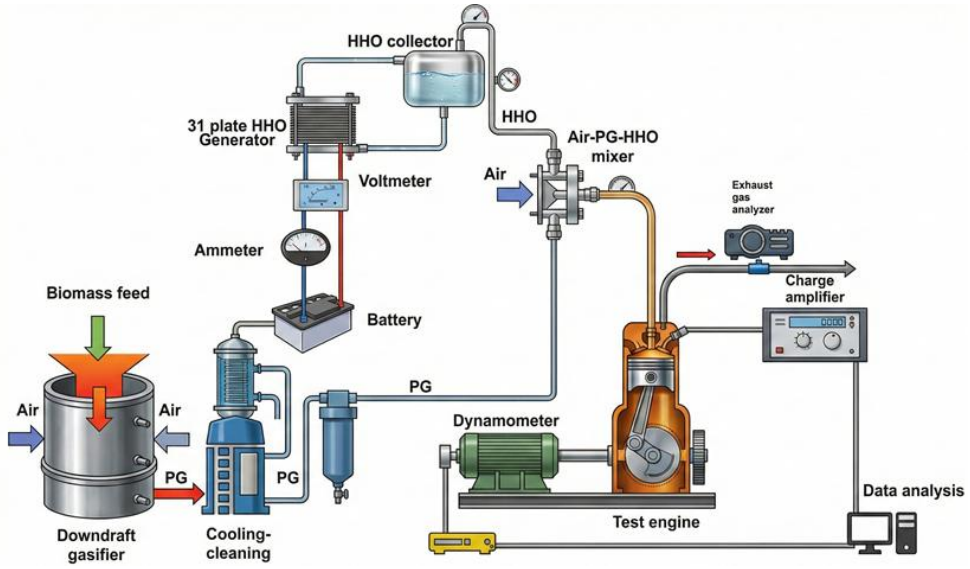

Fig. 1 Engine test setup

Table 2
Test engine specifications

Parameter	Specifications
Engine configuration	Single-cylinder unit
Working cycle	Four-stroke operation
Stroke	110 mm piston travel
Cylinder bore	87.5 mm diameter
Cooling arrangement	Liquid (water) cooling system
Rated brake power	Approximately 3.5 kW
Variable compression ratio range	Adjustable from 12:1 up to 18:1
Dynamometer	AG-10, water-cooled eddy-current dynamometer with separate loading module
Calorimeter type	Coaxial pipe-in-pipe calorimeter
Fuel injector	Electrically actuated solenoid injector
Crank angle encoder	1° crank resolution, up to 5500 rpm, including TDC reference pulse
In-a cylinder pressure sensor	Piezoelectric transducer with 0–350 bar measurement capability
Temperature measurement	RTD PT100 plus K-type thermocouples
Load cell	Strain-gauge sensor, 0–50 kg range
Data acquisition software	"Enginesoft" engine test software
Fuel flow measuring device	DP transmitter, 0–500 mm water column
Cooling water rotameter	Engine jacket flow range: 40–400 LPH
Cooling water pump	Kirloskar monoblock centrifugal pump

consumption, rate of PG flow, rate of intake air flow, electrical power output, and rate of exhaust emission are recorded on the engine side during experiments. HHO gas was generated using a 31-plate water electrolyzer. The process requires a battery power source of 12 VDC and 60 Ah for electricity flow, monitored by an ammeter and voltammeter. A flow meter measures the HHO gas volume flow rate, and a bubbler prevents backfire, assisted by a non-return valve. Safety measures include a flashback arrestor for explosion prevention and a relay connection for automatic switching of the electrolyzer. The system features a resettable circuit breaker for current protection. Fig. 1 depicts the test engine setup. The main specifications of the downdraft gasifier and engine test setup are given in Table 2.

2.5 Response surface methodology

Response Surface Methodology (RSM) is an effective statistical and mathematical model that can be applied in the modeling, analysis, and optimization of processes where one or more input variables affect one or more performance responses. It is specifically useful in the field of engineering and combustion studies, where there are intricate interactions among parameters like injection timing, pilot fuel quantity, gas flow rate, and engine load (Hadiyanto *et al*., 2022; Hoang, Bora, *et al*., 2025). RSM works by fitting a second-order polynomial model between the input factors and the response, and hence both linear and nonlinear effects and interactions of the factors are taken into account (Hadiyat *et al*., 2022; Sarabia & Ortiz, 2009). The Box-Behnken Design (BBD) is one of the several experimental designs employed in the RSM, which is very efficient and is suitable for engine research. BBD uses less experimentation compared to full factorial design or central composite design, does not include any treatment combination where the factors are on the extremes at all times, and the quadratic model is high-quality (Gunst *et al*., 1996; Nazarpour *et al*., 2022). This is optimal when extreme operating conditions can be unsafe or inconvenient, in the case of a study that focuses on optimization of fuel injection or dual-fuel combustion behavior. After the collection of experimental data, the RSM constructed models are compared with the analysis of variance (ANOVA) to identify the statistical significance, interaction, and suitability of the fitted surfaces (Pereira *et al*., 2021; Rejeb *et al*., 2020). To determine the optimal operating point, desirability-based optimization is used, in which all responses (i.e., brake thermal efficiency, NOx emissions, HC, CO, or combustion stability) are converted into desirability functions with values between 0 to 1 (Harrington, 1965; Hoang, Chen, *et al*., 2025). These individual values of desirability are added together to make an overall value of desirability index, indicating the extent to which all optimization objectives are met at the same time. RSM can find the optimum set of engine operating parameters by maximizing this composite desirability to find the best possible trade-off between performance and emissions. Therefore, RSM, Box-Behnken design, together with desirability-based optimization, provides an organized and effective method of optimizing a multi-response engine (Ferreira *et al*., 2007; V. N. Nguyen, Sharma, *et al*., 2023; Sarker *et al*., 2023).

3. Results and discussion

3.1 Engine performance model

The BTE model was developed using RSM RSM-based Box-Behnken model using experimental data. The interactive effect of BMEP, PFIP, and HHO gas flow rate (HHOFR) on the BTE of the dual-fuel engine is shown in Fig. 2. Fig. 2a illustrates the BMEP vs. PFIP contour map. It can be observed that BTE increases gradually with the two parameters (BMEP and PFIP). At a lower BMEP of approximately 1.5 bar and a PFIP of 200 bar, BTE is less than 8% as indicated by the blue to green area. BTE increases up to 28% as the BMEP is near 5.6 bar and the PFIP is near 240 bar, as indicated by the yellow-orange contours. The positive tendency can be explained by the fact that the increase in BMEP increases in-cylinder pressure and temperature, which in turn improves the combustion of PG-air mixtures, and PFIP facilitates the optimization of the atomization and mixing of the pilot diesel (Sharma *et al*., 2022). Fig. 2b confirms this behavior by the corresponding 3D response surface. The inclined plane shows that BTE increases gradually between 8% at the low-BMEP/low-PFIP end to approximately 28% at the high PFIP and higher BMEP. The gradient establishes that there is a very high level of linear-quadratic interaction between the PFIP and BMEP, which indicates that combustion efficiency is very sensitive to the nature of diesel injection during the dual-fuel mode (Halewadimath *et al*., 2023).

The contour map of BMEP vs. HHOFR is depicted in Fig. 3c, where BTE increases with an increase in BMEP; also increase in HHOFR helps in BTE improvement. BTE at HHOFR of 1 LPM is of the order of 8-10 percent at mid-range BMEP

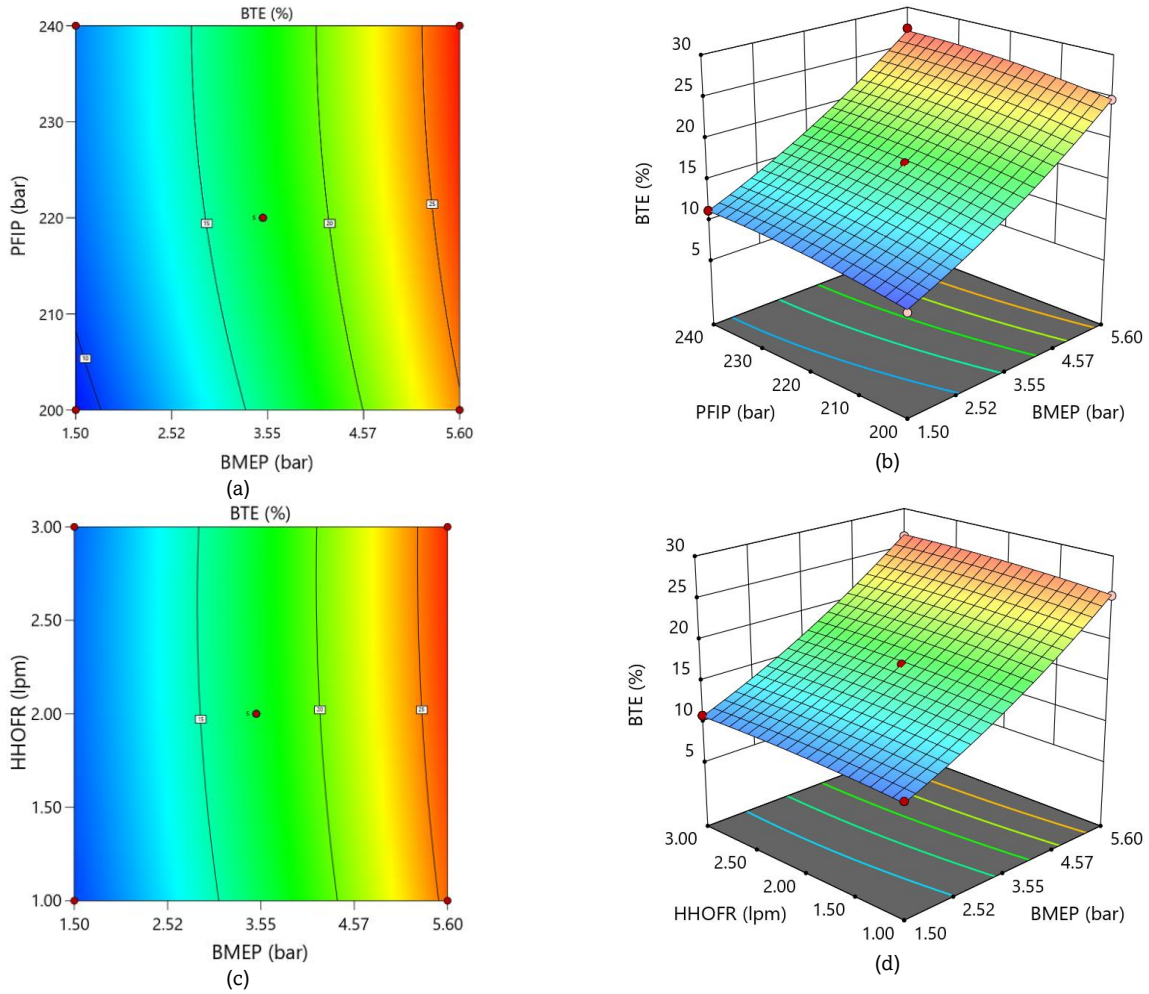

Fig. 2 Response surface plots for the BTE model: (a) contour plot of PFIP vs. BMEP, (b) 3D surface plot of PFIP vs. BMEP, (c) contour plot of HHOFR vs. BMEP, and (d) 3D surface plot of HHOFR vs. BMEP

(approximately 3.5 bar). HHO flow of 3 lpm to 20-25 BTE is enhanced with higher BMEP. This is not surprising since the addition of HHO will accelerate the speed of flames and reduce the time to ignition to allow PG to burn further. As demonstrated in Fig. 3d, the use of increased BMEP and increased HHOFR clearly indicates that BTE is headed to its maximum level (~30%). The dual-fuel combustion process is reinforced by the greater reactivity of the combustion reaction that is afforded by HHO, and the greater the load-dependent thermal efficiency (Dabi & Saha, 2015; Ramadhas *et al.*, 2008).

Table 3 lists the results of ANOVA of BTE and BSEC, which show the statistical significance of the response surface models developed. In both cases, the Model p-value of under 0.0001 confirms that both quadratic models are significant and can be used to explain engine behavior in the course of dual-fuel operation. BMEP (Factor A) has the most significant effect on BTE and BSEC, with the F-values of 7127.93 and 8372.28, respectively. This implies that combustion efficiency and energy use in dual-fuel mode are mostly caused by the variation in load. PFIP (Factor B) is also a significant factor influencing both responses ($p < 0.0001$ BTE; $p = 0.0003$ BSEC), indicating that diesel injection pressure is a crucial factor in stabilizing the ignition and permitting successful combustion of PG. HHOFR (Factor C) has a smaller but statistically significant effect on BTE ($F = 21.31$; $p = 0.0024$) and BSEC ($F = 6.51$; $p = 0.038$), which means that the enrichment with hydrogen plays an important role in enhancing the flame propagation and thermal efficiency. The effects of interaction show that AB (BMEP x PFIP) does not affect BTE but notable effects on BSEC ($p = 0.0054$), which implies that the joint effect of the load and injection pressure has stronger effects on the energy consumption than on thermal efficiency. The interaction terms (AC and BC) are statistically non-significant for both responses, which means that there is not much synergy. Significant quadratic effects A2, B2, and C2 illustrate the nonlinearity of the system, with the dominant A2 curvature effect with F-values of 79.89 (BTE) and 1477.22 (BSEC).

The combined effects of BMEP, PFIP, and HHOFR in relation to Brake Specific Energy Consumption (BSEC) in the dual-fuel mode of operation are shown in Fig. 3. The contour map of BMEP vs. PFIP depicted in Fig. 3a indicates a distinct negative inclination in the BSEC with the increase in both the parameters. The greatest value of BSEC is at low BMEP (1.5 bar) and PFIP (200 bar), with the red-yellow region showing values of nearly 20 to 22 MJ/kWh. BSEC reduces drastically to about 4-6 MJ/kWh as the BMEP hits 5.6 bar and the PFIP gets close to 240 bar, as indicated by the green-blue contours. This is reduced since an increase in BMEP leads to increased efficiency in the working of the load and the relative percentage of pilot fuel needed to maintain steady combustion (Sunil Kumar *et al.*, 2024). Equally, increased PFIP increases atomization, thus better burning of PG, and decreases total energy input per unit work output. This strong downward trend is supported by the 3D response surface in Fig. 3b. The surface is steep with a high BSEC in low-PFIP conditions, with low-load/low-PFIP conditions having a very high BSEC and much lower values

Table 3
ANOVA outcomes for BTE and BSEC

	BTE			BSEC			
Source	**Mean Square**	**F-value**	**p-value**	**Mean Square**	**F-value**	**p-value**	**Remark**
Model	56.22	822.32	< 0.0001	73.61	1093.47	< 0.0001	Significant
A - BMEP	487.34	7127.93	< 0.0001	563.64	8372.28	< 0.0001	
B - PFIP	8.54	124.86	< 0.0001	2.98	44.2	0.0003	
C - HHOFR	1.46	21.31	0.0024	0.4381	6.51	0.038	
AB	0.0119	0.1734	0.6896	1.06	15.78	0.0054	
AC	0.0885	1.29	0.2926	0.0242	0.3596	0.5676	
BC	0.0036	0.0527	0.8251	0.0756	1.12	0.3244	
A^2	5.46	79.89	< 0.0001	99.45	1477.22	< 0.0001	
B^2	1.1	16.05	0.0051	0.2247	3.34	0.1105	
C^2	0.4325	6.33	0.0401	0.7374	10.95	0.0129	
Residual	0.0684	—	—	0.0673	—	—	

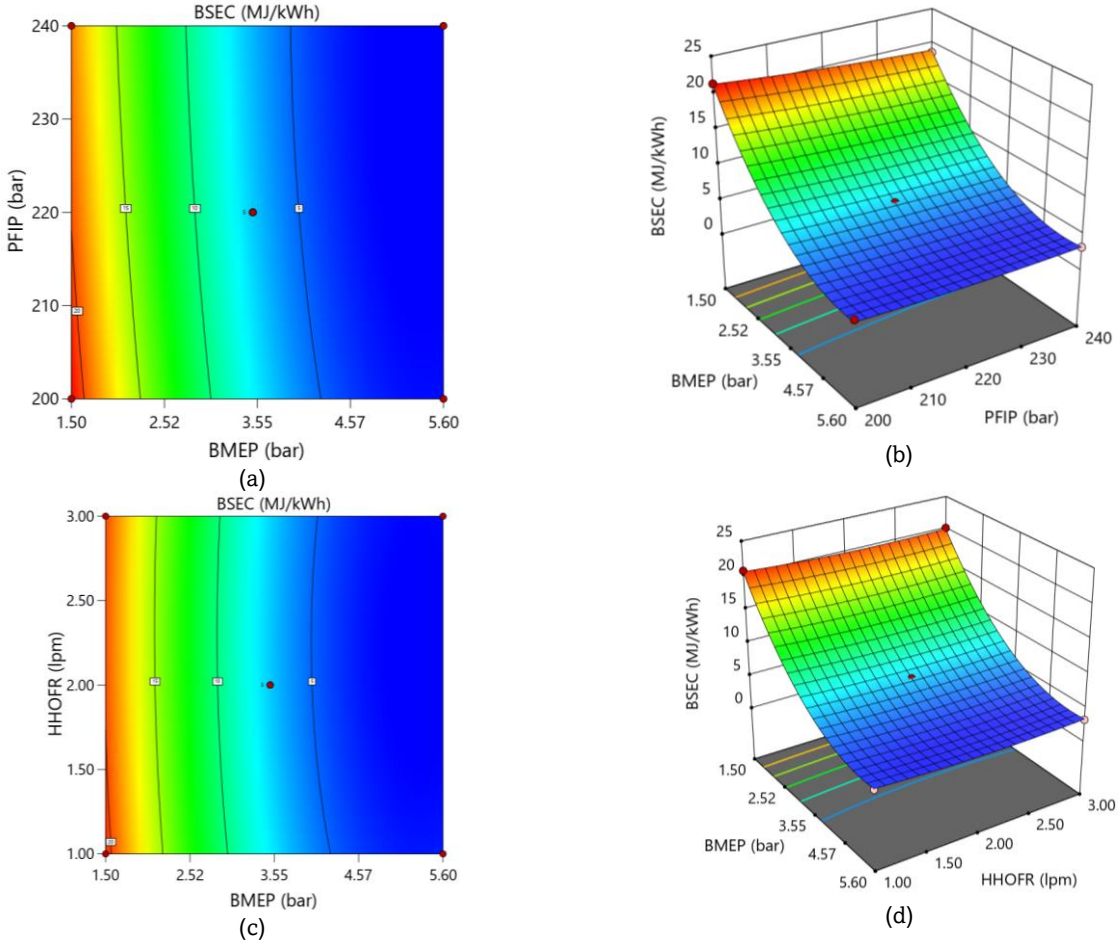

Fig. 3 Response surface plots for the BSEC model: (a) contour plot of PFIP vs. BMEP, (b) 3D surface plot of PFIP vs. BMEP, (c) contour plot of HHOR vs. BMEP, and (d) 3D surface plot of HHOR vs. BMEP

when the BMEP and PFIP are high. It proves that the most powerful factor influencing BSEC is load, and PFIP provides the second, but no less significant, enhancement. The contour diagram BMEP Vs HHoFR of Fig. 3c also shows the same trend. BSEC is reduced to about 20 MJ / kWh at lower levels of BMEP (at lower levels of HHO supply of 1 LPM) to a minimum of 5-7 MJ / kWh at higher levels of BMEP, commonly at levels of 3 LPM HHOFR. HHO improves the efficiency of the combustion since the flame velocity is increased and the ignition delay is reduced, and hence consumes less energy to generate the same brake power. Fig. 4d illustrates a 3D surface, which is a clear indication of the combined effect of increasing BMEP and increasing HHOFR, where BSEC is steadily declining to its minimum value. This establishes that engine load as well as HHO enrichment have a drastic improvement on fuel utilization efficiency during the dual-fuel mode (Subramanian & Thangavel, 2020).

3.2 Engine emission model

Fig. 4 represents the behaviour of carbon monoxide (CO) emission as affected by the rate of BMEP, PFIP, and HHOFR. In the case of CO emissions, BMEP presents a significant effect with an F-value of approximately 225, and the quadratic effect of BMEP is even stronger, as seen by the high F-value of approximately 2556. PFIP also has a significant contribution with an F-value of 22, whereas HHOFR is not very strong, as given in Table 4. Terms of interaction, like combining BMEP

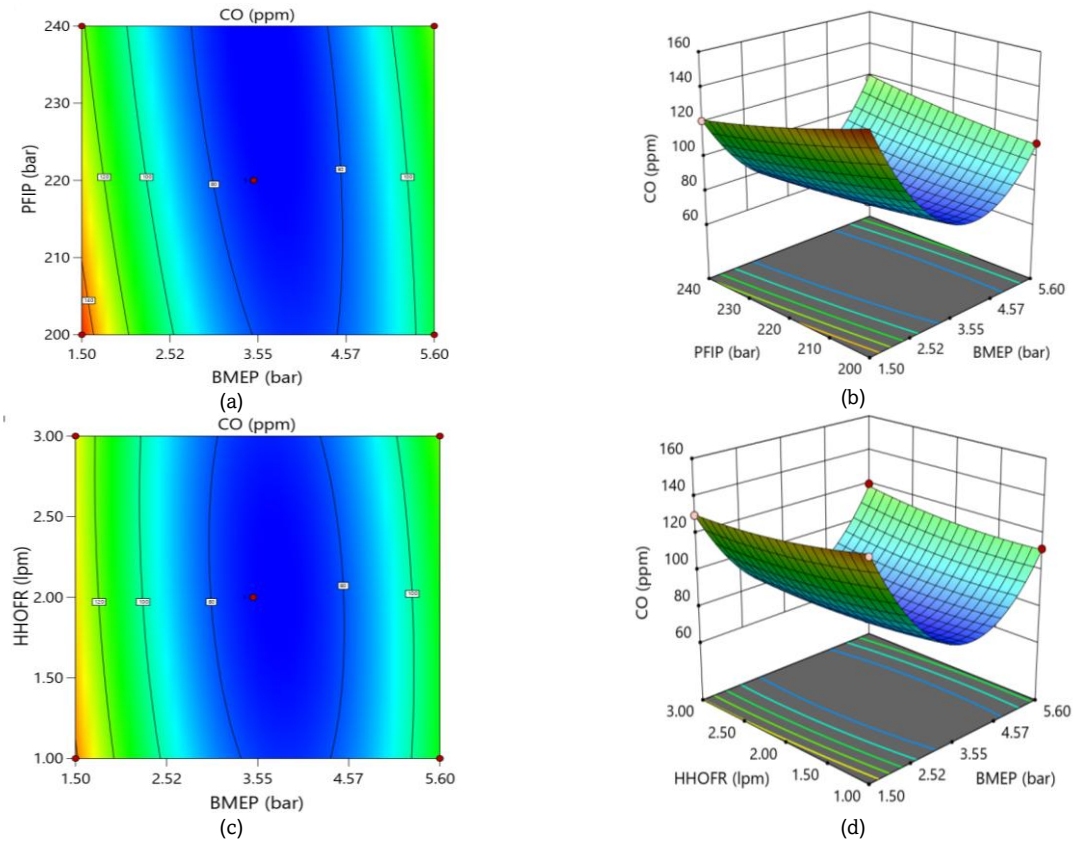

Fig. 4 Response surface plots for the CO emission model: (a) contour plot of PFIP vs. BMEP, (b) 3D surface plot of PFIP vs. BMEP, (c) contour plot of HHOR vs. BMEP, and (d) 3D surface plot of HHOR vs. BMEP

and PFIP and combining BMEP and HHOFR, also exhibit some recognizable effect on CO behaviour. The contour chart (Fig. 4a, BMEP vs. PFIP) indicates that the CO emissions are maximum at the low level of BMEP (around 1.5 bar) and low PFIP (200 bar) with the level of 150ppm and above, as shown in the yellow-green area. With a continued rise in BMEP to 5.6 bar, CO decreases considerably, with the level of CO approaching 50-60 ppm even at moderate PFIP levels (220-230 bar). This decreasing trend is possible as the increased engine load increases the temperature of combustion and the quality of PG oxidation, which results in less unfinished products of combustion, CO. Increasing PFIP also helps in the reduction of CO through the enhancement of the diesel spray atomization, the enhancement of pilot ignition, and piloting the dual-fuel flame (Jain *et al.*, 2023). This reaction is reinforced by the 3D surface shown in Fig. 4b, in which the high CO concentrations observed at low load and low PFIP have a steep downwards slope increasing to much lower values at high BMEP. The curvature is also a pointer to nonlinear interaction, with the leading role being played by BMEP in reducing CO. On the same note, Fig. 4c (BMEP vs. HHOFR) indicates that the CO emissions have a similar trend whereby, at low BMEP and 1 LPM HHO, the emissions are close to 150 ppm, whereas at high BMEP and 3 LPM HHO, the emissions are 50-70 ppm. The inclusion of HHO enhances a quicker flame travel and increases oxidation chemistry because of the availability of hydrogen and oxygen, and allows the PG blend to be fully burned. Fig. 5d indicates that the response surface in 3D is curved, which once again indicates that an increase in BMEP and an increase in HHOFR have a synergistic effect in decreasing CO emissions.

Table 4
ANOVA outcomes for CO, HC, and NOx

Source	CO			HC			NOx			
	Mean Square	F-value	p-value	Mean Square	F-value	p-value	Mean Square	F-value	p-value	Remark
Model	1258.12	329.13	< 0.0001	2719.29	113.33	< 0.0001	9755.58	120.51	< 0.0001	Significant
A - BMEP	861.13	225.27	< 0.0001	1326.12	55.27	0.0001	81810.13	1010.56	< 0.0001	
B - PFIP	84.82	22.19	0.0022	247.43	10.31	0.0148	2436.28	30.09	0.0009	
C - HHOFR	7.14	1.87	0.2139	49.52	2.06	0.194	522.94	6.46	0.0386	
AB	377.53	98.76	< 0.0001	106.03	4.42	0.0736	165.95	2.05	0.1953	
AC	81.42	21.3	0.0024	3.71	0.1547	0.7058	200.06	2.47	0.1599	
BC	0	0	1	0	0	1	1	0.0124	0.9146	
A^2	9770.1	2555.87	< 0.0001	22131.35	922.39	< 0.0001	1496.98	18.49	0.0036	
B^2	15.6	4.08	0.0831	11.81	0.4923	0.5055	624.13	7.71	0.0274	
C^2	42.44	11.1	0.0126	130.87	5.45	0.0522	298.87	3.69	0.0961	
Residual	3.82	—	—	23.99	—	—	80.96	—	—	

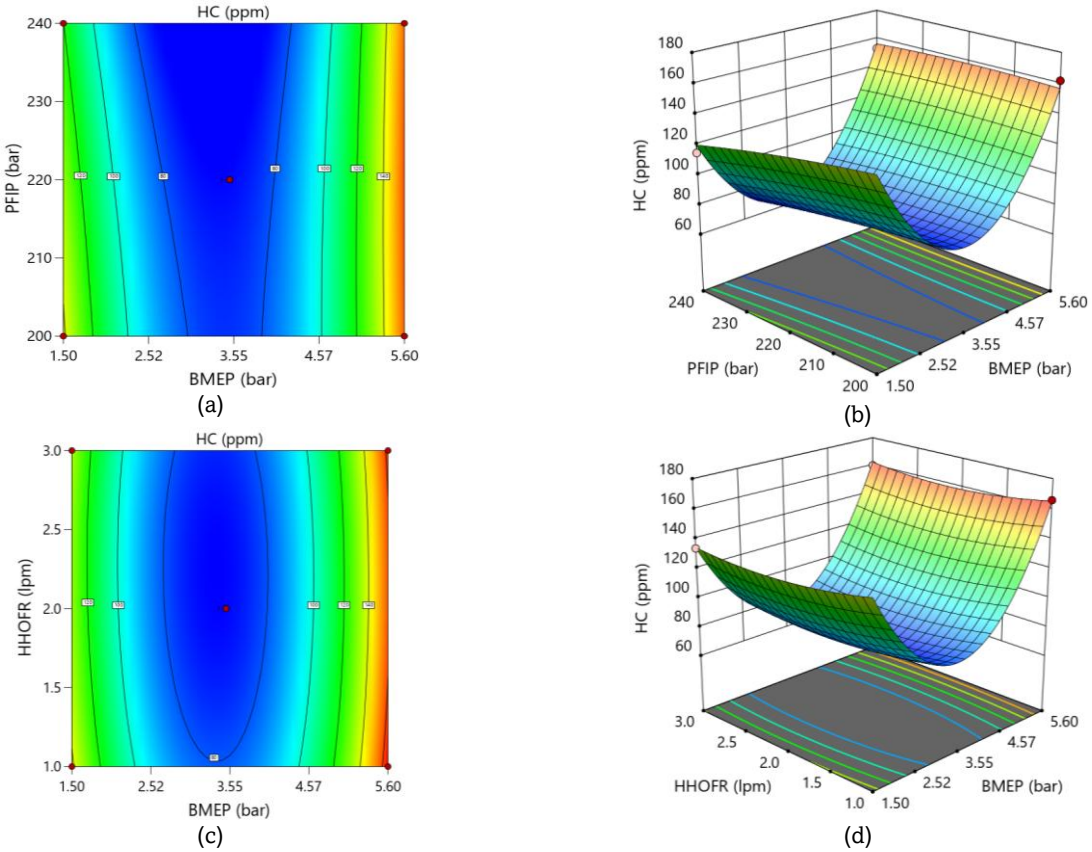

Fig. 5 Response surface plots for the HC emission model: (a) contour plot of PFIP vs. BMEP, (b) 3D surface plot of PFIP vs. BMEP, (c) contour plot of HHOR vs. BMEP, and (d) 3D surface plot of HHOR vs. BMEP

In general, the CO model proves that the benefits of enhancement of the load, increased injection pressure, and hydrogen-enriched combustion play an important role in reducing incomplete combustion emissions in PG-diesel dual-fuel mode.

Fig. 5 illustrates the behaviour of RSM analysis of HC emissions data influenced by the BMEP, PFIP, and HHOFR in a PG-diesel dual-fuel engine. In the case of HC emissions, BMEP comes in once again as a critical variable similar to the previous case of about 55 F-value. PFIP presents an average effect but with an F-value marginally greater than 10 (Table 4). The BMEP quadratic term is significant with an extremely large F-value of approximately 922, showing a strong curvature in the HC response. HHOFR and the majority of interaction effects are not so significant at the same time, as it proves that the HC levels are primarily affected by fluctuations in engine load and fuel-injection-related factors. The contour plot of Fig. 5a (BMEP vs. PFIP) indicates that HC emissions are maximum at the low BMEP (1.5 bar) and both ends of PFIP (200 and 240 bar), and are close to 160-180 ppm. This is anticipated since low engine load creates low in-cylinder temperature as well as insufficient oxidation of PG, which favors unoxidized hydrocarbons. Moreover, both low and high PFIP limit the quality of atomization of fuels, impoverished penetration or excessive penetration of different rates, which results in inefficient air-fuel mixing and combustion envelop (Baruah *et al*., 2021; Bui *et al*., 2021). With further rise of BMEP to 5.6 bar, HC emissions drastically decrease to 60-70 ppm irrespective of PFIP, which is a steep-temperature-dependent decrease in unburned fuel. This trend is validated by the 3D response surface in Fig. 5b, where a concave valley exists at high BMEP, where the HC is minimized. This means that BMEP is the leading determinant that plays a role in the oxidation of the HC as a result of enhanced turbulence and the enhanced mixing in the loads. On the same note, Fig. 5c (BMEP vs. HHOFR) demonstrates that the HC emissions decrease greatly at greater BMEP and intermediate-to-high HHO flow rates. The level of HC decreases to 170 ppm at low BMEP and low HHOFR (1 LPM) to 60 ppm at high BMEP and 3 LPM HHO as a result of the well-known property of hydrogen to increase the speed of flame propagation, reduction of ignition delay, and maximization of the completeness of combustion of PG. A strong downward curvature is also present in the 3D surface in Fig. 5d, with the lowest HC emissions occurring at the combined condition of high BMEP and high HHOFR. In general, the results show that load-induced temperature increase controls the HC emissions positively with the help of optimized pilot injection pressure and hydrogen-assisted combustion that collaboratively minimize the unburnt hydrocarbon formation during dual-fuel work.

The effects of the interaction of BMEP, PFIP, and HHOFR on the NOx emissions in a PG-diesel dual-fuel engine are shown in Fig. 6. The results indicate that high-temperature reaction pathways are determined by thermochemical conditions. The plot of BMEP versus PFIP in Fig. 6a shows that the emissions of NOx are in a constant manner, as the emissions increase with an increase in BMEP, but the rate of increase is not constant, being low at low BMEP (around 1.5 bar) and high at high BMEP (5.6 bar). This behaviour is typical of the Zeldovich thermal-NOx mechanism, in which increased loads increase peak combustion temperature and residence time, which increases the extent of nitrogen oxidation. PFIP also helps in the production of NOx, because an increase in PFIP of 200 to 240 bar enhances better atomization and mixing of pilot diesel and produces a hotter and more uniform flame, and thus better thermal production of NOx. These tendencies are confirmed by the 3D response surface in Fig. 6b. NOx is formed in an ascending plane with growing

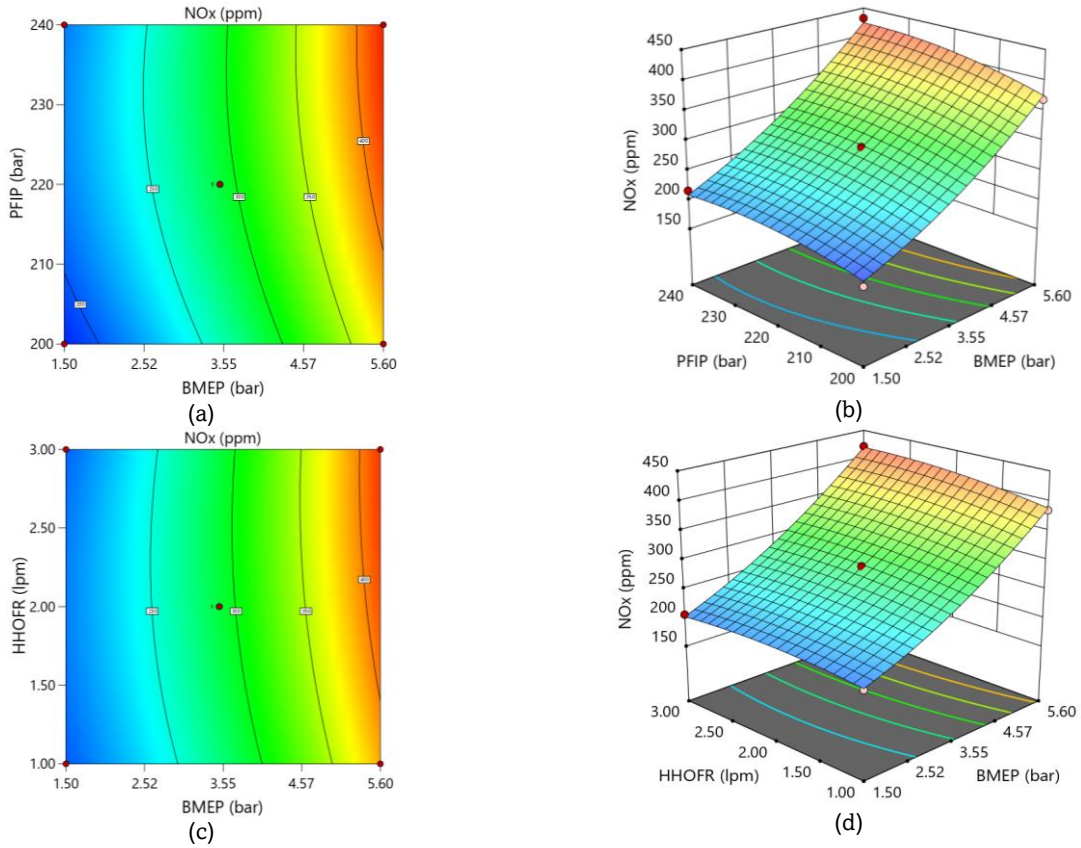

Fig. 6 Response surface plots for the NOx emission model: (a) contour plot of PFIP vs. BMEP, (b) 3D surface plot of PFIP vs. BMEP, (c) contour plot of HHOR vs. BMEP, and (d) 3D surface plot of HHOR vs. BMEP

BMEP and PFIP, with the optimum NOx levels being at the combined state of high BMEP and high PFIP, when the better combustion efficiency is accompanied by higher flame temperatures. On the same note, Fig. 6c (BMEP vs. HHOFR contour) indicates that the emissions of NOx are heavily load-sensitive and sharply rise with the increase in BMEP. HHOFR also has an effect: once the rate of HHO flow has increased to 1, 3 LPM, the level of NOx emissions also increases because the flame speed and adiabatic flame temperature of hydrogen are extremely high, producing a greatly increased effect on the rate of the combustion process of the PG-air mixture. The gradient of the HHOFR axis is, however, lower than the BMEP axis, which means that BMEP is the most important factor of NOx behaviour. The 3D surface in Fig. 6d adds to the evidence of the obvious monotonic increase in NOx with rising BMEP and HHOFR. Peak NOx zone is the combined effect of high load and high hydrogen enrichment that provides favourable conditions in the formation of thermal NOx because of quick oxidation and high in-cylinder temperature profiles. In the case of NOx emission, BMEP has the strongest contribution of 0.1011, indicating how much engine load and combustion temperature are strongly correlated, as decided in Table 4. PFIP also has a significant effect on NOx formation (F-value = 30.09), though HHOFR has a smaller but significant effect (F-value = 6.46). Quadric contributions of BMEP and PFIP also suggest nonlinear changes in NOx formation. The fact that low residual values are obtained in all models confirms that the predictions of the emission are consistent and accurate. On the whole, Fig. 7 shows that, in PG-diesel dual-fuel mode, the temperature-dependent Zeldovich mechanism regulates the emission of NOx, in which high BMEP, optimal diesel injection pressure, and hydrogen-enhanced combustion, all increase the flame temperature and enhance the formation of NOx.

3.3 Desirability-based optimization

As Fig. 7 and Table 5 clearly illustrate, the chosen settings of A (BMEP), B (PFIP), and C (HHOFR) offer a well-optimized increase in performance and emissions. The three are all at the desirability level of one, which confirms that the optimal levels exist as BMEP at 4.23 bar, PFIP at 240 bar, and HHOFR at 2.08 lpm, and fall perfectly inside the most favourable range that the

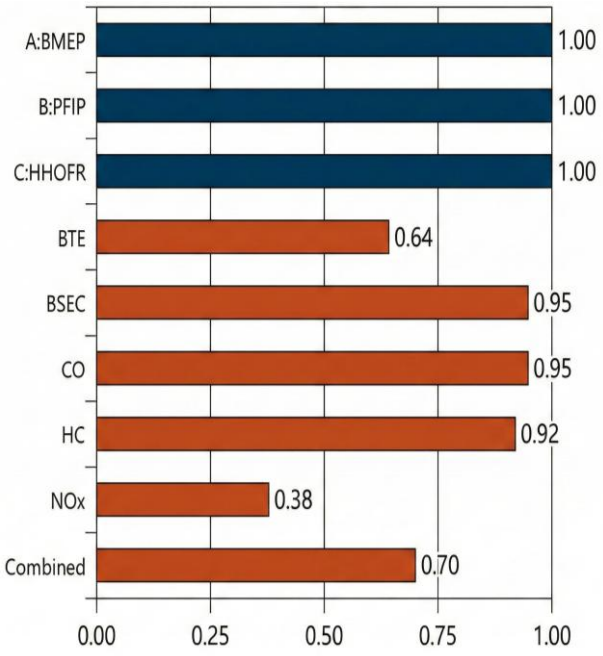

Fig. 7. Desirability bar plot

Table 5
Optimized results

Factor	Name	Level	Coding	Response	Predicted mean	Std Dev	SE mean
A	BMEP, bar	4.23	Actual	BTE, %	20.71	0.26	0.16
B	PFIP, bar	240	Actual	BSEC, MJ/kWh	4.17	0.26	0.16
C	HHOFR, lpm	2.08	Actual	CO, ppm	77.95	1.96	1.22
				HC, ppm	79.47	4.90	3.05
				NOx, ppm	335.99	9.00	5.60

model would recommend. The projected reactions under these levels support the quality of this optimum. BTE has been forecasted to have 20.71 % with a small SD of 0.26, which is why its desirability of 0.64 is moderate. The enhancement in BTE is not so sharp; however, the low uncertainty implies the stable behaviour at the chosen BMEP. On the contrary, BSEC is significantly improved with a predicted value of 4.17 MJ/kWh and SD of 0.26, which is close to its extremely large desirability of 0.95. This establishes the high BMEP and PFIP effectiveness in lowering the unit output of energy. On the emissions side, the CO and HC are significantly improved. CO is estimated at 77.95 ppm and SE at 1.22, which is similar to its high desirability at 0.95. The prediction of HC is 79.47 ppm, with a desirability of 0.92, which implies that HC burns clean at the optimal HHOFR. These findings demonstrate that the selected environments succeed in inhibiting the incomplete-combustion products. In the meantime, NOx, with a predicted value of 335.99 ppm and standard deviation of 9.00, also implies a lower desirability of 0.38, the classic trade-off between low CO and HC, and a slightly higher level of thermal-NOx formation. All in all, the associated desirability of 0.70 represents an effective and viable trade-off considering the significant compromises in BSEC, CO, and HC, with a viable trade-off in the levels of BTE and regulated NOx under the optimality of the operating conditions.

4. Conclusion

The biomass gasification is an important technology that allows the decentralized production of clean energy and especially in areas where agricultural residues are abundantly available. The resultant PG is a renewable alternative to the operation of internal combustion engines, and a small amount of diesel is still good as the pilot fuel needed to get the engine going. This twin fuel approach increases the flexibility of fuel, reduces the use of diesel, and has environmental effects. The current study proves that the optimal choice of operating parameters can contribute greatly to the performance-emission trade-off of producer-gas-diesel engines. BMEP, PFIP, and HHOFR were identified as 4.23 bar, 240 bar, and 2.08 lpm, respectively, as the most optimum operating window, based on the statistical optimization approach. The system under such optimized conditions completes predicted BTE and BSEC of 20.71 % and 4.17 MJ/kWh with relatively low emissions, with CO of 77.95 ppm, HC of 79.47 ppm, and NOx of 335.99 ppm. These findings underscore the importance of a proper regulation of the rate of gas flow and the nature of injection in order to achieve the highest level of combustion stability and the least amount of pollutants. Comprehensively, the research supports the potential of PG and the ideal operation of dual-fuel engines as a viable and long-lasting solution for shifting the energy system towards cleaner energy based on biomass resources.

References

Asadullah, M. (2014). Biomass gasification gas cleaning for downstream applications: A comparative critical review. *Renewable and Sustainable Energy Reviews*, *40*, 118–132. https://doi.org/10.1016/j.rser.2014.07.132

Bandara, W. A. R. T. W., Ranasinghe, O., Perera, P., Vlosky, R., & Kizha, A. R. (2022). Potential to use invasive plants in biomass energy production: A case study Prosopis juliflora in coastal wetlands of Sri Lanka. *Trees, Forests and People*, *10*, 100330. https://doi.org/10.1016/j.tfp.2022.100330

Barik, D., & Murugan, S. (2014). Simultaneous reduction of NOx and smoke in a dual fuel DI diesel engine. *Energy Conversion and Management*, *84*, 217–226. https://doi.org/10.1016/j.enconman.2014.04.042

Baruah, D., Kalita, P., & Moholkar, V. S. (2021). A Comprehensive Study on Utilization of Producer Gas as IC Engine Fuel. In A. . Singh, D. Kumar, & A. . Agarwal (Eds.), *Alternative Fuels and Advanced Combustion Techniques as Sustainable Solutions for Internal Combustion Engines* (pp. 117–147). Springer, Singapore. https://doi.org/10.1007/978-981-16-1513-9_6

Bora, B. J., & Saha, U. K. (2016). Optimisation of injection timing and compression ratio of a raw biogas powered dual fuel diesel engine. *Applied Thermal Engineering*, *92*, 111–121. https://doi.org/10.1016/j.applthermaleng.2015.08.111

Bui, V. G., Bui, T. M. T., Bui, V. H., Vu, M. T., Nguyen, L. C. T., Le, T. T., Ağbulut, Ü., & Hoang, A. T. (2025). Mitigating backfire occurrence in HHO-gasoline plug-in hybrid motorcycle engine. *International Journal of Hydrogen Energy*, *138*, 755–774. https://doi.org/10.1016/j.ijhydene.2025.05.179

Bui, V. G., Bui, T. M. T., Hoang, A. T., Nižetić, S., Nguyen Thi, T. X., & Vo, A. V. (2021). Hydrogen-Enriched Biogas Premixed Charge Combustion and Emissions in Direct Injection and Indirect Injection Diesel Dual Fueled Engines: A Comparative Study. *Journal of Energy Resources Technology*, *143*(12). https://doi.org/10.1115/1.4051574

Caligiuri, C., Renzi, M., Antolini, D., Patuzzi, F., & Baratieri, M. (2021). Diesel fuel substitution using forestry biomass producer gas: Effects of dual fuel combustion on performance and emissions of a micro-CHP system. *Journal of the Energy Institute*, *98*, 334–345. https://doi.org/10.1016/j.joei.2021.07.010

Caligiuri, C., Renzi, M., Antolini, D., Patuzzi, F., & Baratieri, M. (2023). Optimizing the use of forestry biomass producer gas in dual fuel engines: A novel emissions reduction strategy for a micro-CHP system. *Energy Conversion and Management: X*, *20*, 100498. https://doi.org/10.1016/j.ecmx.2023.100498

Chanphavong, L., & Zainal, Z. A. (2019). Characterization and challenge of development of producer gas fuel combustor: A review. *Journal of the Energy Institute*, *92*(5), 1577–1590. https://doi.org/10.1016/j.joei.2018.07.016

Chen, W.-H., & Chen, C.-Y. (2020). Water gas shift reaction for hydrogen production and carbon dioxide capture: A review. *Applied Energy*, *258*, 114078.

Chermprayong, P., Sutheerasak, E., Pirompugd, W., Chuepeng, S., & Sanitjai, S. (2024). *Increasing Flow Rates of Air and Coconut Shell Producer Gas Mixed with PME20 for a Diesel Engine Generator* (pp. 285–293). https://doi.org/10.1007/978-3-031-49787-2_26

Dabi, M., & Saha, U. K. (2015, December). Experimental Analysis of a Dual-Fuel Engine Fueled by Producer Gas Derived From Pine Leaves and Cattle Dung Briquettes. *ASME 2015 Gas Turbine India Conference*. https://doi.org/10.1115/GTINDIA2015-1263

Dai, H., Zhao, H., Chen, S., & Jiang, B. (2021). A Microwave-Assisted Boudouard Reaction: A Highly Effective Reduction of the Greenhouse Gas CO2 to Useful CO Feedstock with Semi-Coke. *Molecules*, *26*(6), 1507. https://doi.org/10.3390/molecules26061507

Das, S., Kanth, S., Das, B., & Debbarma, S. (2022). Experimental evaluation of hydrogen enrichment in a dual-fueled CRDI diesel

engine. *International Journal of Hydrogen Energy*, *47*(20), 11039–11051. https://doi.org/10.1016/j.ijhydene.2022.01.125

Das, S., Kashyap, D., Kalita, P., Kulkarni, V., & Itaya, Y. (2020). Clean gaseous fuel application in diesel engine: A sustainable option for rural electrification in India. *Renewable and Sustainable Energy Reviews*, *117*, 109485. https://doi.org/10.1016/j.rser.2019.109485

Ferreira, S. L. C., Bruns, R. E., Ferreira, H. S., Matos, G. D., David, J. M., Brandão, G. C., da Silva, E. G. P., Portugal, L. A., dos Reis, P. S., Souza, A. S., & dos Santos, W. N. L. (2007). Box-Behnken design: An alternative for the optimization of analytical methods. *Analytica Chimica Acta*, *597*(2), 179–186. https://doi.org/10.1016/j.aca.2007.07.011

Freda, C., Catizzone, E., Villone, A., & Cornacchia, G. (2024). Biomass gasification in rotary kiln integrated with a producer gas thermal cleaning unit: An experimental investigation. *Results in Engineering*, *21*, 101763. https://doi.org/10.1016/j.rineng.2024.101763

Ghodke, P., & Mandapati, R. N. (2019). Investigation of particle level kinetic modeling for babul wood pyrolysis. *Fuel*, *236*, 1008–1017. https://doi.org/10.1016/j.fuel.2018.09.084

Gunst, R. F., Myers, R. H., & Montgomery, D. C. (1996). Response Surface Methodology: Process and Product Optimization Using Designed Experiments. *Technometrics*, *38*(3), 285. https://doi.org/10.2307/1270613

Hadiyanto, H., Christwardana, M., Pratiwi, W. Z., Purwanto, P., Sudarno, S., Haryani, K., & Hoang, A. T. (2022). Response surface optimization of microalgae microbial fuel cell (MMFC) enhanced by yeast immobilization for bioelectricity production. *Chemosphere*, *287*, 132275. https://doi.org/10.1016/j.chemosphere.2021.132275

Hadiyat, M. A., Sopha, B. M., & Wibowo, B. S. (2022). Response Surface Methodology Using Observational Data: A Systematic Literature Review. *Applied Sciences*, *12*(20), 10663. https://doi.org/10.3390/app122010663

Halewadimath, S. S., Banapurmath, N. R., Yaliwal, V. S., Gaitonde, V. N., Khan, T. M. Y., Vadlamudi, C., Krishnappa, S., & Sajjan, A. M. (2023). Experimental Investigations on Dual-Fuel Engine Fueled with Tertiary Renewable Fuel Combinations of Biodiesel and Producer—Hydrogen Gas Using Response Surface Methodology. *Sustainability*, *15*(5), 4483. https://doi.org/10.3390/su15054483

Halewadimath, S. S., Yaliwal, V. S., Banapurmath, N. R., & Sajjan, A. M. (2020). Influence of hydrogen enriched producer gas (HPG) on the combustion characteristics of a CRDI diesel engine operated on dual-fuel mode using renewable and sustainable fuels. *Fuel*, *270*, 117575. https://doi.org/10.1016/j.fuel.2020.117575

Harrington, E. C. (1965). The desirability function. *Industrial Quality Control*, *21*(10), 494–498.

Havilah, P. R., Sharma, A. K., Govindasamy, G., Matsakas, L., & Patel, A. (2022). Biomass Gasification in Downdraft Gasifiers: A Technical Review on Production, Up-Gradation and Application of Synthesis Gas. *Energies*, *15*(11), 3938. https://doi.org/10.3390/en15113938

Hoang, A. T. (2019). Experimental study on spray and emission characteristics of a diesel engine fueled with preheated bio-oils and diesel fuel. *Energy*, *171*, 795–808. https://doi.org/10.1016/j.energy.2019.01.076

Hoang, A. T. (2024). Critical review on the characteristics of performance, combustion and emissions of PCCI engine controlled by early injection strategy based on narrow-angle direct injection (NADI). *Energy Sources, Part A: Recovery, Utilization, and Environmental Effects*, *46*(1), 13791–13805. https://doi.org/10.1080/15567036.2020.1805048

Hoang, A. T., Bora, B. J., Huynh, D. N. L., Nguyen, D. K. P., & Le, V. V. (2025). Dual-fuel diesel engine features powered by ammonia under various pilot-fuel injection timing: Comprehensive analysis and response surface methodology-based optimization. *International Journal of Engine Research*. https://doi.org/10.1177/14680874251341036

Hoang, A. T., Chen, W. H., Paramasivam, P., Kanti, P. K., Huynh, D. N. L., Abdou El-Shafay, A. S., & Nguyen, V. Q. (2025). Comprehensive investigation on performance and emission of dual-fuel diesel engine fuelled with biodiesel and hydrogen using D-optimal design and desirability-based multi-attribute optimization. *International Journal of Hydrogen Energy*, *146*, 150005. https://doi.org/10.1016/J.IJHYDENE.2025.06.195

Huang, Wan, Liu, Zhang, Ma, Zhang, & Zhou. (2019). A Downdraft Fixed-Bed Biomass Gasification System with Integrated Products of Electricity, Heat, and Biochar: The Key Features and Initial Commercial Performance. *Energies*, *12*(15), 2979. https://doi.org/10.3390/en12152979

Huynh, D. N. L., Hoang, A. T., Nayak, S. K., Guerrero-Pérez, M. O., Rodríguez-Castellón, E., López-Escalante, M. C., Sănduleac, M., Efremov, C., Bui, V. G., Luu, V. C., Nguyen, X. P., & Cao, D. N. (2025). Combining Babool wood-derived producer gas and hydrogen with biodiesel as efficient strategies for dual-fuel diesel engine in advancing sustainable energy. *Case Studies in Thermal Engineering*, *75*, 107097. https://doi.org/10.1016/J.CSITE.2025.107097

Jain, A., Jyoti Bora, B., Kumar, R., Sharma, P., Jyoti Medhi, B., Ahsan Farooque, A., Tirth, V., Senthilkumar, N., & Kumar Peyyala, P. (2023). Impact of titanium dioxide (TiO2) nanoparticles addition in Eichhornia Crassipes biodiesel used to fuel compression ignition engine at variable injection pressure. *Case Studies in Thermal Engineering*, *49*, 103295. https://doi.org/10.1016/j.csite.2023.103295

Khandal, S. V., Ağbulut, Ü., Afzal, A., Sharifpur, M., Abdul Razak, K., & Khalilpoor, N. (2022). Influences of hydrogen addition from different dual-fuel modes on engine behaviors. *Energy Science & Engineering*, *10*(3), 881–891. https://doi.org/10.1002/ese3.1065

Krop, N. S., & Brito, P. (2023). A Review on Gaseous Fuels for Dual-Fuel Diesel Engines. In *Proceedings of the 2nd International Conference on Water Energy Food and Sustainability (ICoWEFS 2022)* (pp. 386–395). Springer International Publishing. https://doi.org/10.1007/978-3-031-26849-6_40

Lahijani, P., Zainal, Z. A., Mohammadi, M., & Mohamed, A. R. (2015). Conversion of the greenhouse gas CO2 to the fuel gas CO via the Boudouard reaction: A review. *Renewable and Sustainable Energy Reviews*, *41*, 615–632. https://doi.org/10.1016/j.rser.2014.08.034

Le, T. T., Balasubramanian, D., Le, A. T., Cao, D. N., Chen, W.-H., Venugopal, I. P., Ağbulut, Ü., Truong, T. H., Nguyen, X. P., Bui, V. G., & Hoang, A. T. (2025). Partially-charged advanced low-temperature combustion in diesel engine: Progress and prospects. *Alexandria Engineering Journal*, *129*, 373–440. https://doi.org/10.1016/j.aej.2025.06.021

Le, T. T., Sharma, P., Le, H. C., Le, H. S., Osman, S. M., Truong, T. H., Le, D. T. N., Rowinski, L., & Tran, V. D. (2024). A glass-box approach for predictive modeling based on experimental data for a waste biomass derived producer gas-powered dual-fuel engine. *International Journal of Hydrogen Energy*, *58*, 1122–1137. https://doi.org/10.1016/j.ijhydene.2024.01.284

Liu, H., Wang, Z., Long, Y., Xiang, S., Wang, J., & Wagnon, S. W. (2015). Methanol-gasoline Dual-fuel Spark Ignition (DFSI) combustion with dual-injection for engine particle number (PN) reduction and fuel economy improvement. *Energy*, *89*, 1010–1017. https://doi.org/10.1016/j.energy.2015.06.051

Ma, L., Zhang, G., Liu, A., Zheng, J., Shao, Y., Ding, X., Gao, P., & Li, Q. (2026). Unexpected Increase in Tail Gas Greenhouse Effect of Diesel Vehicles Equipped with Advanced Post-Treatment Systems. *Separation and Purification Technology*, *381*, 135617. https://doi.org/10.1016/j.seppur.2025.135617

Monteiro, E., Ramos, A., & Rouboa, A. (2024). Fundamental designs of gasification plants for combined heat and power. *Renewable and Sustainable Energy Reviews*, *196*, 114305. https://doi.org/10.1016/j.rser.2024.114305

Nayak, B., Singh, T. J., & Hoang, A. T. (2021). Experimental analysis of performance and emission of a turbocharged diesel engine operated in dual-fuel mode fueled with bamboo leaf-generated gaseous and waste palm oil biodiesel/diesel fuel blends. *Energy Sources, Part A: Recovery, Utilization, and Environmental Effects*, 1–19. https://doi.org/10.1080/15567036.2021.2009595

Nazarpour, M., Taghizadeh-Alisaraei, A., Asghari, A., Abbaszadeh-Mayvan, A., & Tatari, A. (2022). Optimization of biohydrogen production from microalgae by response surface methodology (RSM). *Energy*, *253*, 124059. https://doi.org/10.1016/j.energy.2022.124059

Nguyen, P. Q. P., Tran, V. D., Nguyen, D., Luong, C. N., & Paramasivam, P. (2025). Application of response surface methodology to

optimize the dual-fuel engine running on producer gas. *International Journal of Renewable Energy Development*, *14*(2), 214–223. https://doi.org/10.61435/ijred.2025.60927

Nguyen, T. B. N., & Le, N. V. L. (2023). Biomass resources and thermal conversion biomass to biofuel for cleaner energy: A review. *Journal of Emerging Science and Engineering*, *1*(1), 6–13. https://doi.org/10.61435/jese.2023.2

Nguyen, V. G., Tran, M. H., Paramasivam, P., Le, H. C., & Nguyen, D. T. (2024). Biomass: A Versatile Resource for Biofuel, Industrial, and Environmental Solution. *International Journal on Advanced Science, Engineering and Information Technology*, *14*(1), 268–286. https://doi.org/10.18517/ijaseit.14.1.17489

Nguyen, V. N., Nayak, B., Singh, T. J., Nayak, S. K., Cao, D. N., Le, H. C., & Nguyen, X. P. (2023). Investigations on the performance, emission and combustion characteristics of a dual-fuel diesel engine fueled with induced bamboo leaf gaseous fuel and injected mixed biodiesel-diesel blends. *International Journal of Hydrogen Energy*. https://doi.org/10.1016/j.ijhydene.2023.06.074

Nguyen, V. N., Sharma, P., Kumar, A., Pham, M. T., Le, H. C., Truong, T. H., & Cao, D. N. (2023). Optimization of biodiesel production from Nahar oil using Box-Behnken design, ANOVA and grey wolf optimizer. *International Journal of Renewable Energy Development*, *12*(4), 711–719. https://doi.org/10.14710/ijred.2023.54941

Oduor, N. M., & Githiomi, J. K. (2013). Fuel-wood energy properties of Prosopis juliflora and Prosopis pallida grown in Baringo District, Kenya. *African Journal of Agricultural Research 8*(21), 2476–2481. https://doi.org/10.5897/AJAR08.221

Palani, Y., Devarajan, C., Manickam, D., & Thanikodi, S. (2020). Performance and emission characteristics of biodiesel-blend in diesel engine: A review. *Environmental Engineering Research*, *27*(1), 200338–0. https://doi.org/10.4491/eer.2020.338

Patra, T. K., & Sheth, P. N. (2015). Biomass gasification models for downdraft gasifier: A state-of-the-art review. *Renewable and Sustainable Energy Reviews*, *50*, 583–593. https://doi.org/10.1016/j.rser.2015.05.012

Percy, A. J., & Edwin, M. (2023). Studies on the performance and emission characteristics of a dual fuel VCR engine using producer gas as secondary fuel: An optimization approach using response surface methodology. *Energy*, *263*, 125685. https://doi.org/10.1016/j.energy.2022.125685

Pereira, L. M. S., Milan, T. M., & Tapia-Blácido, D. R. (2021). Using response surface methodology (RSM) to optimize 2G bioethanol production: a review. *Biomass and Bioenergy*, *151*, 106166.

Phrommarat, B., & Arromdee, P. (2025). Comparative life cycle assessment of pelletized biomass fuels from corncobs and rubberwood sawdust. *International Journal of Renewable Energy Development*, *14*(4), 740–750. https://doi.org/10.61435/ijred.2025.61011

Prabhahar, M., Prakash, S., Nallusamy, S., Ponnarasu, S., & Reddy, Y. D. (2024). Optimization of Operating Factors and Blending Levels of Diesel, Algae Methyl Ester, Graphene Oxide and Producer Gases - Calorific Values Using Response Surface Methodology in HCCI Engine. *International Journal of Mechanical Engineering*, *11*(1), 1–15. https://doi.org/10.14445/23488360/IJME-V11I1P101

Prajapati, L. K., & Tirkey, J. V. (2025). Effect of injection pressure and nozzle strategy optimization for the performance improvement on CI engine fuelled with diesel and co-gasified biomass producer gas: A diesel-RK and RSM-based approach. *Process Safety and Environmental Protection*, *198*, 107197. https://doi.org/10.1016/j.psep.2025.107197

Prajapati, L. K., Tirkey, J. V., Jena, P., & Giri, A. (2024). Parametric performance evaluation of SI engine using producer gas-biogas-hydrogen blend as a fuel: A thermodynamic modeling and optimization approach. *International Journal of Hydrogen Energy*, *72*, 268–287. https://doi.org/10.1016/j.ijhydene.2024.05.386

Raj, R., Tirkey, J. V., Jena, P., & Prajapati, L. K. (2024). Comparative analysis of Gasifier-CI engine performance and emissions characteristics using diesel with producer gas derived from coal–briquette-coconut shell-mahua feedstock and its blends. *Energy*, *293*, 130708. https://doi.org/10.1016/j.energy.2024.130708

Ramadhas, A. S., Jayaraj, S., & Muraleedharan, C. (2008). Dual fuel mode operation in diesel engines using renewable fuels: Rubber seed oil and coir-pith producer gas. *Renewable Energy*, *33*(9), 2077–2083. https://doi.org/10.1016/j.renene.2007.11.013

Raman, P., Ram, N. K., & Gupta, R. (2013). A dual fired downdraft gasifier system to produce cleaner gas for power generation: Design, development and performance analysis. *Energy*, *54*, 302–314. https://doi.org/10.1016/j.energy.2013.03.019

Rejeb, O., Ghenai, C., Jomaa, M. H., & Bettayeb, M. (2020). Statistical study of a solar nanofluid photovoltaic thermal collector performance using response surface methodology. *Case Studies in Thermal Engineering*, *21*, 100721. https://doi.org/10.1016/j.csite.2020.100721

Reyes, M., Pérez, J. F., & Sastre, R. (2024). Combustion performance and flame front morphology of producer gas from a biomass gasification-based cookstove. *Fuel*, *362*, 130763. https://doi.org/10.1016/j.fuel.2023.130763

Santana, H. E. P., Jesus, M., Santos, J., Rodrigues, A. C., Pires, P., Ruzene, D. S., Silva, I. P., & Silva, D. P. (2025). Lignocellulosic Biomass Gasification: Perspectives, Challenges, and Methods for Tar Elimination. *Sustainability*, *17*(5), 1888. https://doi.org/10.3390/su17051888

Sarabia, L. A., & Ortiz, M. C. (2009). Response Surface Methodology. *Comprehensive Chemometrics*, *1*(2), 345–390. https://doi.org/10.1016/B978-044452701-1.00083-1

Sarker, T. R., Nanda, S., & Dalai, A. K. (2023). Parametric studies on hydrothermal gasification of biomass pellets using Box-Behnken experimental design to produce fuel gas and hydrochar. *Journal of Cleaner Production*, *388*, 135804. https://doi.org/10.1016/j.jclepro.2022.135804

Sharma, P., & Bora, B. J. (2023). Modeling and optimization of a CI engine running on producer gas fortified with oxyhydrogen. *Energy*, *270*, 126909. https://doi.org/10.1016/j.energy.2023.126909

Sharma, P., Chhillar, A., Said, Z., Huang, Z., Nguyen, V. N., Nguyen, P. Q. P., & Nguyen, X. P. (2022). Experimental investigations on efficiency and instability of combustion process in a diesel engine fueled with ternary blends of hydrogen peroxide additive/biodiesel/diesel. *Energy Sources, Part A: Recovery, Utilization, and Environmental Effects*, *44*(3), 5929–5950. https://doi.org/10.1080/15567036.2022.2091692

Sharma, P., Sahoo, B. B., Said, Z., Hadiyanto, H., Nguyen, X. P., Nižetić, S., Huang, Z., Hoang, A. T., & Li, C. (2023). Application of machine learning and Box-Behnken design in optimizing engine characteristics operated with a dual-fuel mode of algal biodiesel and waste-derived biogas. *International Journal of Hydrogen Energy*, *48*(18), 6738–6760. https://doi.org/10.1016/j.ijhydene.2022.04.152

Sharma, P., Sharma, A. K., & Ağbulut, Ü. (2025). A comprehensive review on biomass-derived producer gas as an alternative fuel: a waste biomass-to-energy perspective. *Journal of Thermal Analysis and Calorimetry*, *150*(12), 8913–8932. https://doi.org/10.1007/s10973-025-14292-8

Shu, Z., Gan, H., Ji, Z., & Liu, B. (2022). Modeling and Optimization of Fuel-Mode Switching and Control Systems for Marine Dual-Fuel Engine. *Journal of Marine Science and Engineering*, *10*(12), 2004. https://doi.org/10.3390/jmse10122004

Singh, P., Kumar, R., Sharma, S., & Kumar, S. (2021). Effect of engine parameters on the performance of dual-fuel CI engines with producer gas—a review. *Energy & Fuels*, *35*(20), 16377–16402.

Smith R J, B., Loganathan, M., & Shantha, M. S. (2010). A Review of the Water Gas Shift Reaction Kinetics. *International Journal of Chemical Reactor Engineering*, *8*(1). https://doi.org/10.2202/1542-6580.2238

Stettler, M. E. J., Midgley, W. J. B., Swanson, J. J., Cebon, D., & Boies, A. M. (2016). Greenhouse Gas and Noxious Emissions from Dual Fuel Diesel and Natural Gas Heavy Goods Vehicles. *Environmental Science & Technology*, *50*(4), 2018–2026. https://doi.org/10.1021/acs.est.5b04240

Subramanian, B., & Thangavel, V. (2020). Experimental investigations on performance, emission and combustion characteristics of Diesel-Hydrogen and Diesel-HHO gas in a Dual fuel CI engine. *International Journal of Hydrogen Energy*, *45*(46), 25479–25492. https://doi.org/10.1016/j.ijhydene.2020.06.280

Sunil Kumar, K., Surakasi, R., Patro, S. G. K., Govil, N., Ramis, M. K., Razak, A., Sharma, P., Alsubih, M., Islam, S., Khan, T. M. Y., Almakayeel, N., & Chintakindi, S. (2024). Performance, Combustion, and Emission analysis of diesel engine fuelled with

pyrolysis oil blends and n-propyl alcohol-RSM optimization and ML modelling. *Journal of Cleaner Production*, *434*, 140354. https://doi.org/10.1016/j.jclepro.2023.140354

Susastriawan, A. A. P., Saptoadi, H., & Purnomo. (2017). Small-scale downdraft gasifiers for biomass gasification: A review. *Renewable and Sustainable Energy Reviews*, *76*, 989–1003. https://doi.org/10.1016/j.rser.2017.03.112

Sutar, K. B., Kohli, S., & Ravi, M. R. (2023). Clean cooking with downdraft biomass gasifier cookstove: Effect of gasifier performance. *Energy*, *263*, 125631. https://doi.org/10.1016/j.energy.2022.125631

Thomson, R., Kwong, P., Ahmad, E., & Nigam, K. D. P. (2020). Clean syngas from small commercial biomass gasifiers; a review of gasifier development, recent advances and performance evaluation. *International Journal of Hydrogen Energy*, *45*(41), 21087–21111. https://doi.org/10.1016/j.ijhydene.2020.05.160

Tulu, T. K., Atnaw, S. M., Bededa, R. D., Wakshume, D. G., & Ancha, V. R. (2022). Kinetic Modeling and Optimization of Biomass Gasification in Bubbling Fluidized Bed Gasifier Using Response Surface Method. *International Journal of Renewable Energy Development*, *11*(4), 1043–1059. https://doi.org/10.14710/ijred.2022.45179

Veza, I., Afzal, A., Mujtaba, M. A., Tuan Hoang, A., Balasubramanian, D., Sekar, M., Fattah, I. M. R., Soudagar, M. E. M., EL-Seesy, A. I., Djamari, D. W., Hananto, A. L., Putra, N. R., & Tamaldin, N. (2022). Review of artificial neural networks for gasoline, diesel and homogeneous charge compression ignition engine. *Alexandria Engineering Journal*, *61*(11), 8363–8391. https://doi.org/10.1016/j.aej.2022.01.072

Winangun, K., Setiyawan, A., & Sudarmanta, B. (2023). The combustion characteristics and performance of a Diesel Dual-Fuel (DDF) engine fueled by palm oil biodiesel and hydrogen gas. *Case Studies in Thermal Engineering*, *42*, 102755. https://doi.org/10.1016/j.csite.2023.102755

Zhang, Z., Dong, R., Lan, G., Yuan, T., & Tan, D. (2023). Diesel particulate filter regeneration mechanism of modern automobile engines and methods of reducing PM emissions: a review. *Environmental Science and Pollution Research*, *30*(14), 39338–39376. https://doi.org/10.1007/s11356-023-25579-4